



Cite this: DOI: 10.1039/d5fb00685f


Received 14th October 2025  
Accepted 2nd February 2026

DOI: 10.1039/d5fb00685f

rsc.li/susfoodtech

Microscopy is an indispensable scientific imaging tool that is used for the magnified visualization of diverse kinds of cells, cellular structures and post-labelled molecules for various microbiological, diagnostic and biomedical applications. Conventionally, for microscopic imaging, specimens are often mounted or fixed onto glass slides with or without covering them with glass coverslips. However, both these components are brittle, chemically inert, involve expensive and sophisticated manufacturing, and possess razor-sharp edges that pose safety hazards, causing blood borne disease transmission *via* accidental cuts under clinical scenarios. In response to the growing need for sustainable and safe laboratory materials, we developed a transparent, biodegradable bio-slide processed from pristine fish-scale bio-wastes. This is an extension of our previous study, where we utilized the transparency of the scale for UV-vis spectroscopy. Rich in collagen and hydroxyapatite, the scales were subjected to controlled demineralization and bio-casting to yield slide-comparable optically clear bio-slides with a mechanical strength of  $\sim 40 \pm 4$  mPa. The bio-slides demonstrated consistent ( $n = 10$ ) light transmittance (over 82%), acceptable autofluorescence, solvent compatibility and enhanced sample adherence with a contact angle of  $81^\circ$ , supporting imaging of a broad range of specimen (plant parts and tissue sections, bacteria, and cells). As conventional microscopes are designed to stage “slides”, a customized reusable 3D-printed slide-mimicking adapter was developed to position our bio-slide on the microscope. The bio-slide could withstand laser excitation, permitting imaging using confocal microscopy, and showed high-compatibility towards dyes (Synap-toRed C2, DAPI, crystal violet, and safranin) and antibody-labels (anti-NeuN antibody and Alexa 555-conjugated secondary antibody (goat anti-mouse IgG1)) enabling microbial and cell staining and immunohistochemistry of mice spinal cord neuronal sections (20  $\mu\text{m}$  and 30  $\mu\text{m}$ ). Finally, the renewable and biodegradable nature of the bio-slide supports circular bio-economy goals through effective bio-waste

## Sustainable development of pellucid bio-slides from discarded fish scales for microscopy imaging

M. E. Amal,<sup>†a</sup> K. P. Paul David,<sup>†a</sup> Aishwarya D. Bantupalli,<sup>†a</sup> Elna B. Kuriappuram,<sup>†a</sup> Ambika Ray,<sup>†a</sup> Venkata Sruthi Kadiyala,<sup>a</sup> Jemi Feiona Vergil Andrews,<sup>a</sup> Salman Khan,<sup>a</sup> Chiranjeevi Korupalli,<sup>a</sup> Vengala Rao Yenuganti,<sup>a</sup> G. B. Madhubabu,<sup>b</sup> Pitchaiah Cherukuri,<sup>a</sup> Divya S. Parimi<sup>a</sup> and Anil K. Suresh <sup>\*a</sup>

### Sustainability spotlight

A sustainable and biodegradable alternative to conventional glass slides used in microscopy is presented by valorizing discarded fish-scale bio-waste into a functional bio-slide with optical and mechanical properties comparable to commercial glass, enabling safer laboratory practices by integrating biowaste valorization, green material design, and safety innovation for a greener scientific ecosystem.

valorisation. This study introduces an eco-friendly class of bio-slides for imaging using microscopy with promising applications in green diagnostics, sustainable laboratory practices, and biomedical research.

## 1 Introduction

Microscopy is an extremely essential imaging technique that is widely used in hospitals, diagnostic and research laboratories for high-resolution visualization of structures and intricate cellular and physiological processes beyond the limit of the human naked eye.<sup>1,2</sup> Its application spans across various domains including cell biology, microbiology, materials science and pathology, where microscopes ranging from conventional light microscopes to advanced microscopes such as fluorescence, confocal, and stimulated emission depletion (STED) have become indispensable for elucidating subcellular dynamics, biological structures, pathological conditions, and driving innovations in microbiology, diagnosis and biomedicine.<sup>3-5</sup> The microscopy of diverse samples is typically visualized by mounting or fixing the specimen onto the gold standard “glass-slide” based on the interaction of light beams with a specimen to produce a magnified image, facilitating the detailed examination of cellular architecture, microorganisms and tissue morphology, their differentiation *etc.*<sup>6-8</sup>

Glass slides, while widely used in microscopy, present several pressing limitations that can affect imaging quality and experimental outcomes. Additionally, glass may exhibit autofluorescence under specific imaging conditions, such as

<sup>a</sup>Department of Biological Sciences, SRM University-AP, Amaravati-522503, India. E-mail: anil.s@srmmap.edu.in; Tel: +91 9440968970

<sup>b</sup>Department of Biotechnology and Bioinformatics, University of Hyderabad, Hyderabad-500046, India

<sup>†</sup> Equal contribution.



fluorescence microscopy, leading to background noise and reduced signal-to-noise ratio.<sup>9,10</sup> The chemical resistance of glass is also limited, as certain solvents or reagents may cause etching or degradation of the glass surface, making imaging difficult.<sup>11,12</sup> Furthermore, repeated cleaning and reuse can result in surface scratches, reducing sample adhesion and optical performance over time. Most importantly, their inherent fragility and razor-sharp edges make them highly vulnerable to breakage and accidental piercing, posing great risks to the clinical practitioners.<sup>13,14</sup> Such incidents not only result in physical wounds but also raise serious concerns regarding occupational transmission of infectious agents (e.g. hepatitis B, human immunodeficiency virus), particularly in diagnostic, pathology and microbiology labs handling biohazardous samples. Reports from laboratory personnel document deep cuts caused by accidental slide breakage during routine tasks, underscoring the slide's sharpness even after chemical staining procedures.<sup>15</sup> Additionally, environmental health and safety offices report cases where broken glass, including slides, has led to eye injuries and blood exposure incidents.<sup>16</sup> These injuries are recognized as sharps-related accidents, prompting the need for strict disposal protocols and the use of forceps or puncture-resistant containers.<sup>17</sup> The frequent occurrence of such accidents highlights the urgent need for safer, biodegradable alternatives to conventional glass slides, particularly those made from bio-waste derived materials that eliminate sharp edges and fragility while maintaining optical pellucidity.

Preferably, sourcing functional materials from bio-waste aligns with the Sustainable Development Goals (SDGs) of preserving both the green and blue economies.<sup>18</sup> Biological scaffolds inherently exhibit properties suited for specific applications, making them highly attractive for sustainable material development.<sup>19,20</sup> Among such bio-wastes, fish scales, discarded in millions of tons globally, stand out due to their compelling optical, semi-absorptive, mechanical, metal-binding, oxido-reductive, and electronic characteristics rooted in their collagenous chemical composition.<sup>21</sup> These properties have enabled their use in diverse applications, including television displays, piezoelectric nanogenerators, heavy metal remediation, wound healing, low-volume spectroscopy<sup>22</sup> and self-degrading prosthetic implants.<sup>23</sup> Given the significant land occupancy, disposal costs, environmental hazards, and risk of pathogen propagation associated with unmanaged fish scale bio-waste, the responsible valorization of scales is a matter of utmost global priority.<sup>24,25</sup> Moreover, fish scale derivatives are naturally biodegradable, making them inherently green and environmentally sustainable.<sup>21,31</sup>

Herein, we present fish scale waste as a biodegradable bio-slide for microscopy, leveraging its inherent transparency (over 82%), hydrophilicity and superior specimen-retention capability.<sup>32</sup> Because conventional optical microscopes are optimized for standard glass slides, we fabricated a customized, reusable 3D-printed adapter to securely accommodate our bio-slide onto the microscope stage. The bio-slide exhibited outstanding structural integrity under laser excitation and exceptional compatibility to common dyes and labelling agents, thereby facilitating high-resolution confocal imaging of cells

and tissues. This performance is attributed to its superior optical transmittance across the visible and fluorescence range (350–900 nm). In addition, the bio-slide proved compatible while imaging bacteria, transverse sections of plant leaves and stems, pollen, and staining protocols to enable fluorescence immunohistochemistry on mouse spinal cord sections, all visualized with clarity and diagnostic relevance. Notably, unlike glass, which is prone to etching and degradation in non-polar solvents, the bio-slide remained chemically stable. This innovation not only provides a sustainable alternative to traditional glass slides but also highlights a transformative approach to repurposing food waste into functional platforms for routine microscopy.

## 2 Materials and methods

### 2.1. Materials

Fish scales of rohu (*Labeo rohita*) having an average diameter of ~12–18 mm were brought from the local fish market. Staining dyes were purchased from Himedia Ltd India. *E. coli* and *S. aureus* were purchased from Microbial Culture Collection, CSIR-NCL, Pune, India. All other chemicals and reagents were from standard commercial sources and of the highest quality available.

### 2.2. Animal experiments

C57BL/6NCRl mice were procured from Hylasco Biotechnology Pvt. Ltd, Hyderabad, India. Mice were housed under a 12 h light–dark cycle with food and water provided *ad libitum* at the Central Animal Facility, University of Hyderabad, India. Mice used in this study were part of another experiment (3R principle). All the animal experiments were conducted in accordance with the Institutional Animal Ethical Committee (IAEC) approval (UH/IAEC/MGB/2023-1/05) and under the regulations of the Committee for the Purpose of Control and Supervision of Experiments on Animals (CPCSEA), India.

**2.2.1. Perfusion, fixation, cryo-blocking and sectioning of the tissues.** The animals were deeply anesthetized with a cocktail of ketamine and xylazine and were transcardially perfused with 1 × phosphate buffer saline (PBS), followed by 4% paraformaldehyde (PFA). The spinal cord was dissected and fixed in 4% PFA at 4 °C for an additional 2 h. After fixation, spinal cord tissues were gently washed in 1 × PBS at room temperature – 3 times@2 h each. The tissues were then transferred to 20% sucrose solution and incubated at 4 °C until the tissues were completely sunk. Eventually, the spinal roots were carefully peeled, and lumbar segments were embedded using OCT compound in Peel-A-Way embedding molds. The blocks were frozen using liquid nitrogen (N<sub>2</sub>)=cooled isopentane and were stored at –80 °C until further use. From the prepared spinal cord cryo-blocks, spinal cord sections (20 μm and 30 μm) were obtained using a Leica cryostat and the sections were directly collected onto nitrocellulose-coated bio-slides. The slides were stored at either –20 °C or at 4 °C until further use.

**2.2.2. Immunohistochemistry.** The bio-slides with tissue sections were taken in a 12-well plate (single section per well)



and were processed for immunohistochemistry. The bio-slides with spinal cord cross-sections were washed three times in  $1 \times$  PBS (10 minutes each wash). The sections were then incubated overnight at  $4\text{ }^{\circ}\text{C}$  with primary antibody (anti-NeuN antibody 1 : 200 dilution; cat. #MAB377 Chemicon) diluted in blocking solution (2% BSA, 0.5% Triton X-100 in  $1 \times$  PBS). Following incubation with primary antibody, the bio-slides with sections were washed thrice in  $1 \times$  PBS (10 minutes each wash). Then the sections were incubated with Alexa 555-conjugated secondary antibody (goat anti-mouse IgG1) for 2.5 h at RT. After incubation, the sections were washed thrice in  $1 \times$  PBS (10 minutes each wash). The sections were then mounted with glass coverslips (mounting medium 50% glycerol in  $1 \times$  PBS) and prepared for confocal microscopy by placing them in a customized 3D printed adapter. For regular fluorescence microscopy, we used a rapid protocol for immunohistochemistry. All washes with  $1 \times$  PBS were similar to the protocol mentioned above for confocal microscopy. The incubation with primary antibodies was for 5 h at  $32\text{ }^{\circ}\text{C}$  and it was 2 h for the secondary antibodies. After final PBS washes, the sections were mounted with a glass coverslip using Mowiol as mounting medium and were imaged on a Nikon Eclipse Ti2 microscope.

### 2.3. Valorization of pellucid bio-slides from discarded fish scales

Fish scales were first gently rubbed with Milli-Q water to remove surface mucopolysaccharides and other debris. They were then subjected to a sequential etching process involving rocking at 200 rpm in 50 mL of 1 M NaOH, followed by treatment with 50 mL of 10% HCl at room temperature for 1 h to achieve demineralization and decellularization. Afterward, the scales were soaked overnight in Milli-Q water for further purification and then air-dried for 24 h to obtain a transparent scale. Following each treatment stage, the scales were rinsed thoroughly with Milli-Q water using mild friction. After attaining a transmittance of over 82%, the scales were uniformly cut into  $1\text{ cm} \times 1\text{ cm}$  pieces, hereafter designated as “bio-slide,” using scissors, and were stored in sealed, airtight containers until future use.

### 2.4. Assessing the pellucidity, surface architecture and wettability of the bio-slide

To assess optical pellucidity (absorbance and transmittance), UV-vis spectra of the bio-slide were recorded using a multi-scanner sky spectrophotometer (Thermo Scientific, California, USA) operating at a wavelength resolution of 1 nm. A custom-designed adapter developed by us<sup>22</sup> was used to securely position the bio-slide for accurate measurements of the thin film.

Optical pellucidity and surface morphological appearance of the bio-slide were further evaluated using an Olympus Microscope CKX53 (Olympus, Tokyo, Japan) installed with a Magcam MU2A camera.

Static and time-domain wettability measurements of our bio-slide by drop casting  $5\text{ }\mu\text{L}$  of sessile droplets were performed using a contact angle goniometer (HO-IAD-CAM-01, Holmarc, India). Contact angle values were obtained from recorded

videos using ImageJ software by drop shape analysis. All the measurements were carried out at least in triplicate to ensure reproducibility.

Tensile strength is measured using a universal testing machine (2D Strain Master-LaVision, Germany) with a 100 N load cell and a frame capacity of 1 kN at a cross head speed of  $6\text{ mm min}^{-1}$ .

### 2.5. Design and 3D printing of a reusable bio-slide holder

The bio-slide, being a  $1\text{ cm} \times 1\text{ cm}$  expendable piece, was fitted into a re-usable slide-like support with a holding groove in the middle, which was designed and printed using polylactic acid material *via* a 3D printer (Fig. 3).

### 2.6. Visualization of the bacteria on the-bio-slide

As a proof-of-concept, slide comparable imaging potential of the bio-slide was first assessed using the smallest living creatures on the planet. Briefly,  $5\text{ }\mu\text{L}$  each of the two morphologies; rods (*Escherichia coli*) and spheres (*Staphylococcus aureus*) of bacteria having an optical density of 0.6 were placed in the middle of the bio-slides, spread gently using a pipette tip for air-drying. The bio-slides were immediately placed in the groove of the slide support to mount them onto the stage of the microscope for imaging at different magnifications.

### 2.7. Exploitation of the bio-slide to image biogenic macro-structures and tissue sections

For the real-time microscopy observations,  $5\text{ }\mu\text{L}$  each of various samples, including trans-sectioned plant leaves and stem, pollen, and eukaryotic cells (HeLa and MBA-MB-231 cell lines), were placed separately in the middle of the bio-slide, spread across gently using the tip, and the bio-slide was carefully placed on the groove of the slide-support using forceps while facing the droplet upwards suitable for microscopy.

### 2.8. Staining compatibility of the bio-slide

The staining compatibility test of the bio-slide was performed using a bio-slide Gram staining assay.<sup>26</sup> First,  $5\text{ }\mu\text{L}$  of the bacteria is air-dried on the bio-slide to form a bacterial smear on the bio-slide. Then, the bio-slide is flooded with crystal violet, followed by Gram's iodine to fix the primary stain. Next, we applied a decolorizer to remove the dye from Gram-negative cells. Finally, a counterstain, safranin, is applied to stain the decolorized cells pink, allowing observation of the purple Gram-positive and pink Gram-negative bacteria under a microscope upon drying.

### 2.9. Microscopy and image quantification

Compatibility assessment of our bio-slide for laser confocal microscopy was performed by imaging immune-stained mouse spinal cord cross sections on a confocal microscope (LSM 710, Carl Zeiss, Germany) in brightfield mode to locate the region of interest. Once the region was focused, the system was switched to confocal mode. Imaging parameters such as pinhole size, laser power, photomultiplier gain, and signal offset were



carefully adjusted to optimize image quality and minimize photobleaching and signal saturation. The sections were scanned sequentially with laser excitation appropriate for Alexa 555 to capture high-resolution fluorescence images. The sections were also visualized under transmitted light microscopic field. All the images were captured at various magnifications using the Carl Zeiss software. Regular fluorescence imaging was performed on a Nikon Eclipse Ti2 microscope. For auto-fluorescence intensity measurements, similar gain and exposure settings were used for image acquisition. Image quantification was performed using Fiji software.<sup>37</sup> All quantifications were performed on raw images (.nd2 files).

### 3 Results and discussion

Biological matrices inherently possess diverse structural and functional attributes that, when thoughtfully adapted, can be translated into useful applications for human benefit.<sup>27,28</sup> Leveraging the natural pellucidity and hydrophilicity of fish scales, this study extends the valorization of discarded fish scales into transparent bio-slides for microscopy imaging. This innovation pioneers a sustainable alternative to conventional glass slides, which, due to their fragility and sharp edges, are prone to breakage and accidental injury, causing disease (hepatitis B, human immunodeficiency virus *etc.*) transmission *via* accidental cuts, posing significant risks to clinical practitioners.<sup>29</sup> Etched fish scales that were transformed into bio-slides demonstrated excellent optical transparency and hydrophilicity, enabling their direct use in microscopy with the aid of a 3D-printed slide-mimicking holder, as the bio-slides are 1 cm × 1 cm pieces.

As a proof-of-concept, comparative imaging studies of diverse samples mounted on bio-slides exhibited clarity and resolution on par with conventional glass slides, confirming their suitability for diverse microscopic applications. A schematic illustration of the transformation of discarded fish scale bio-wastes into highly transparent bio-slides suitable for multiplexed microscopy of diverse species, including prokaryotic and eukaryotic cells and tissue transverse sections, is given in Fig. 1. Additionally, the bio-slides facilitated staining-based monitoring of cells and tissues using confocal microscopy *in situ*, withstanding exposure to laser excitation, underscoring their potential as eco-friendly and versatile platforms for high-resolution microscopy, and microbiological and clinical diagnostics.

The collagenous and mineral-rich composition of scales likely contributes to their transparency and rigidity when processed, thereby mimicking the performance of glass.<sup>30</sup> Importantly, the use of bio-slides introduces a sustainable alternative by valorizing aquaculture waste into a functional laboratory material. This not only reduces reliance on energy-intensive glass production but also addresses waste management challenges through biodegradability.<sup>31</sup> While the current results validate their compatibility with routine microscopy. Further improvements in uniformity and durability could expand their utility in high-throughput and advanced imaging platforms. Beyond safety, this approach also aligns with the broader

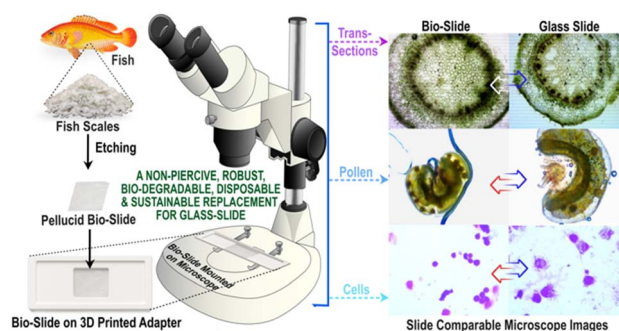


Fig. 1 Scheme illustrating the development of fish scales into pellucid bio-slides for glass slide comparable microscopy. (a) Design and development of highly transparent bio-slides upon etching the scales and a 3D printed holder to place the bio-slide. (b) Mounting of the bio-slide onto the slide-holder of the microscope for capturing images. Right panel: comparative microscopy images of plant stem sections, pollen grains, and stained eukaryotic cells mounted on bio-slides and glass slides, demonstrating comparable optical clarity and resolution.

imperative of fostering environmentally stable and sustainable practices.

#### 3.1. Derivation of pellucid bio-slide, morphological and optical characterization

After thoroughly washing using Milli-Q water to remove the surface monosaccharides, sand and other debris, subsequent base and acid etching of intact fish scales led to their decellularization and demineralization attaining the inner transparent corneal stromal lamellar skeleton, named “bio-slide”. Etching treatment thinned the fish scales from  $\sim 0.425 \text{ mm} \pm 0.025 \text{ mm}$  to  $\sim 0.11 \pm 0.02 \text{ mm}$ , obtained by measuring 50 samples using a screw gauge (Fig. S5), elevating their high transparency and uniformity. The evolution of see-through transparency increased gradually with every etching step as reflected by the clearer appearance of the label “BIO-SLIDE” placed underneath (Fig. 4c). The etching is not restricted to *Labeo rohita*, and the bio-slide could be produced using scales of other fish species such as *Catla catla* and *Clupea ilisha* (Fig. S9).

For the validation of the bio-slides for microscopy experiments, their surface architecture was examined using epifluorescence microscopy. Pristine bio-slide samples showed naturally patterned structures (Fig. 2a), likely originating from the collagenous hierarchy of fish scales, while the glass slide (Fig. 2d) displayed a smooth and featureless surface. Despite these minute structural differences, optical characterization confirmed comparable performance between bio-slides and glass slides. These ridges were so small ( $\sim 45\text{--}75 \text{ nm}$ ) and did not interfere or impact with any of the specimen imaging and or staining performed. The UV-vis absorption spectra (Fig. 2e) showed that bio-slides possess negligible absorbance in the visible region (350–900 nm), similar to glass, ensuring minimal background interference during imaging. Correspondingly, transmittance spectra (Fig. 2f) demonstrated that bio-slides achieve high transparency across the visible wavelength range, with transmission values of over 82%, nearly overlapping those



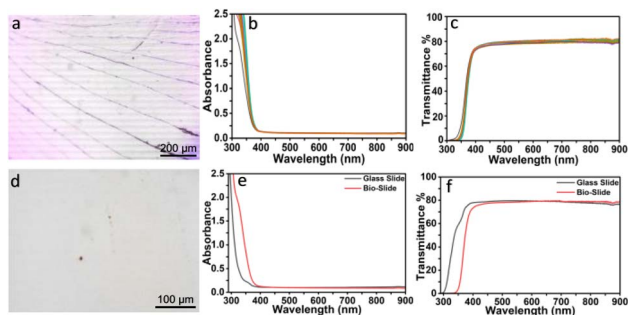


Fig. 2 Optical and surface characterization of bio-slides versus conventional glass slides. (a and d) Epi-fluorescence microscopy images showing the surface morphology of bio-slides (a) and glass slides (d). UV-vis absorption spectra (b) and transmittance (c) of bio-slides, showing negligible absorbance in the visible region. Comparative absorbance (e) and transmittance (f) of the bio-slide vs. glass slide, confirming high optical transparency comparable to glass slides.

of conventional glass slides. These results collectively validate that bio-slides retain the optical clarity necessary for microscopy, effectively transmitting light without distortion or significant scattering. The intrinsic biomolecular composition of fish scales, comprising hydroxyapatite and collagen, likely contributes to their optical performance when processed.<sup>30</sup> Importantly, this work emphasizes that such bio-waste-derived substrates can match the quality of standard glass slides while offering the added advantage of sustainability, biodegradability, and reduced environmental impact. Future refinements in surface polishing and uniformity could further enhance their consistency, positioning bio-slides as reliable eco-friendly alternatives for routine laboratory and educational microscopy.

### 3.2. Sample drop-cast ability of the pellucid bio-slide

Specimen drop-cast potential of the bio-slide, as measured using contact angle, revealed that the bio-slide is hydrophilic with a contact angle of 81° (Fig. 3a). The wettability of the bio-slide as a function of time demonstrated a decrease in contact angle from 83° to 81° within 2 min, after which the angle remained constant (Fig. 3a). To accommodate the imaging of non-aqueously suspended specimen, the bio-slides were coated

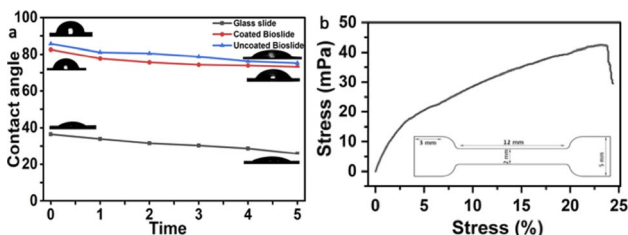


Fig. 3 Contact angle and mechanical strength analysis of bio-slides. (a) Wettability measurements of bio-slides versus glass slides over time, showing that glass slides (~40°) are more hydrophilic than bio-slides compared to nitrocellulose uncoated bio-slides (~81°). Nitrocellulose coated bio-slides exhibited intermediate wettability (~79°). (b) Tensile strength measurements of Cu<sub>2</sub>O@biotemplate with tensile specimen orientation and geometry as the dog bone standard (inset).

with 40% nitrocellulose, and doing so did not reflect their contact angle (Fig. 3a). The bio-slide showed high mechanical strength, with a tensile strength of  $\sim 40 \pm 4$  mPa (Fig. 3b), due to hierarchically oriented collagen fibres and hydroxyapatite within the mineralized layers of fish scales (Fig. 3b). This high tensile strength and malleable nature ensured stability against mechanical shear and tear during sample processing for diverse microscopic observations. Together, these features make our bio-slide compatible for the microscopic observation of rare, solvent-compatible (Fig. S7), hydrophobic and hydrophilic sample specimens.

### 3.3. Design and 3D printing of a reusable bio-slide holder

As our bio-slide is a 1 cm × 1 cm piece, to ensure compatibility with standard microscopy infrastructure, a custom 3D-printed holder was designed (Fig. 4). This holder is re-usable with a holding groove in the middle to fit the bio-slide (Fig. 4a). The schematic shows the cross-sectional and dimensional layout, enabling the holder to mimic the footprint of a conventional glass slide. The bio-slide holding position on the support was marked exactly in the middle of the slide-like support so that it can be securely mounted onto the stage of the microscope and falls in the centre of the objective. This design overcomes the variability in scale size and geometry, ensuring reliable integration without requiring instrumentation modifications.

### 3.4. On bio-slide imaging of diverse biological specimens

The compatibility and suitability of the bio-slide for microscopy imaging was first validated by observing the bacteria. We carefully picked rod shaped Gram-negative (*E. coli*) and spherical shaped Gram-positive (*S. aureus*) bacteria (Fig. 5a–d) so as to infer that diverse species and shapes of bacteria can be visualized. Another reason for picking two distinctly far species is to establish non-interference of our bio-slide to various biological staining procedures in this case exposure to crystal violet and safranin, confirming that standard biological staining and imaging workflows remain unaffected (Fig. 5). To our prediction, the bio-slide worked flawlessly by capturing images of

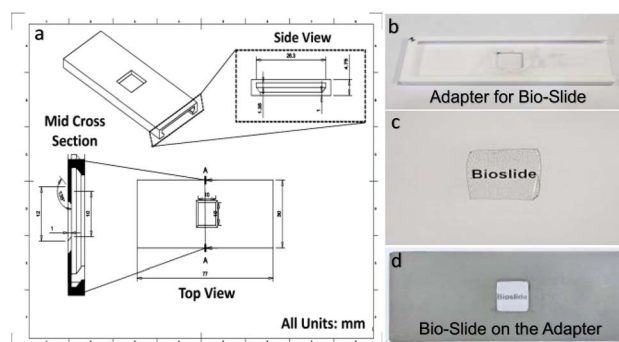
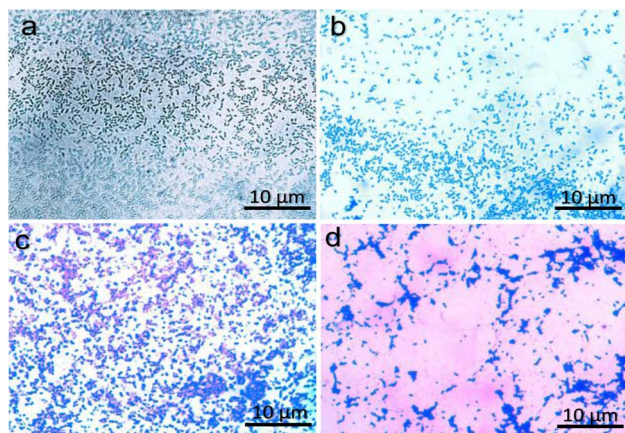


Fig. 4 Design and 3D-printing of slide-like holder for bio-slides. (a) Schematic representation showing cross-sectional, side, and top views of the holder. (b) Fabricated adapter mimicking the footprint of a conventional glass slide. (c) Processed bio-slide. (d) Bio-slide mounted on the holder for microscopy.





**Fig. 5** Microscopic visualization of rod-shaped and spherical bacteria on bio-slides and glass slides. Representative micrographs showing the morphology of rod-shaped bacteria (*E. coli*) on the bio-slide (a) and the glass slide (b) and spherical bacteria (*S. aureus*) on the bio-slide (c) and the glass slide (d). Both bacterial types displayed well-preserved morphology, clear cellular outlines, and sharp contrast, confirming that bio-slides provide imaging performance comparable to glass substrates.

bacteria that were comparable to similar imaging on glass slides (Fig. 5a–d).

Having learned that our bio-slide can be used for microscopy, to validate its diversified use in imaging we exploited the bio-slide further to visualize other higher organisms. Representative micrographs demonstrated that the plant leaf section (Fig. 6a), plant stem section (Fig. 6c), and pollen grain structure (Fig. 6e) could be clearly visualized with excellent contrast and resolution comparable to similar imaging on typical glass slides (Fig. 6b, d and f). As can be inferred transverse sections of different plant parts can be clearly visualized using our bio-slide.

Likewise, our bio-slide showed high compatibility to visualize, examine and capture different eukaryotic cell lines including MDA-MB-231 (Fig. 7) and HeLa (Fig. S8), and with different staining dyes such as SynaptoRed C2 to stain

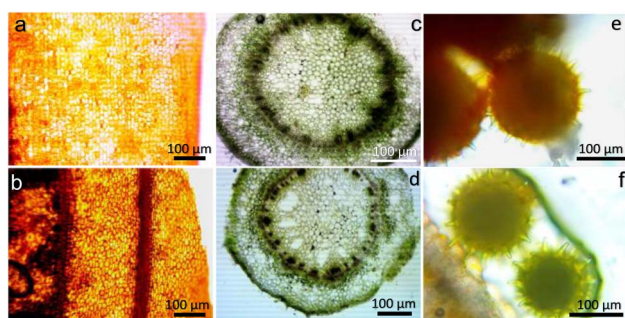


**Fig. 6** Microscopic imaging of different transverse sections of plant parts on bio-slides in comparison to glass slides. Representative micrographs of the plant leaf section (a), plant stem section (c), and pollen grain structure (e) compared to similar imaging on typical glass slides (b, d and f).

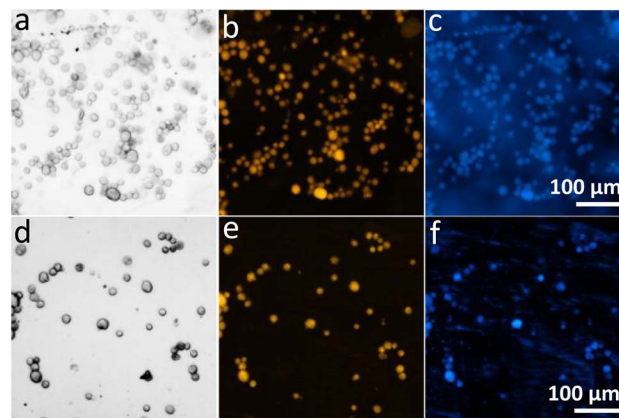


**Fig. 7** Microscopic images of eukaryotic cell lines on bio-slides and glass slides. Images showing MDA-MB-231 under bright field (a), SynaptoRed C2 (b) and DAPI (c) on bio-slides and glass slides (d–f) under similar conditions, displaying imaging and staining compatibility and cellular outlines comparable to those of glass slides.

cytoplasm and DAPI to visualize nuclei for wider exploitation of our bio-slide (Fig. 7 and S8). Different staining protocols produced sharp cellular outlines, well-defined structures, and minimal background interference, validating the ability of bio-slides to support *in vitro* cell imaging. All specimens were visualized with high clarity and contrast, on par with glass slides, confirming the compatibility of bio-slides with diverse microscopy applications.

To further validate the potential of bio-slides for fluorescence microscopy, we performed fluorescence immunohistochemistry on mouse spinal cord cross sections and imaged them using a confocal laser scanning microscope. Autofluorescence measurements of bio-slides in different channels – UV (excitation: 377.5 nm; emission: 457.5 nm), FITC (excitation: 475 nm; emission: 535 nm), and TRITC (excitation: 550 nm; emission: 603.5) – when compared with glass slides were slightly higher but were within an acceptable range (Fig. S11) and did not affect the image quality (Fig. 7 and 8). Even though bio-slides showed slightly higher autofluorescence as compared to glass slides, this would be taken care of during image analysis, wherein background subtraction will result in corrected fluorescence intensities.

Immunohistochemistry assessments reveal that the spinal cord sections have adhered well to the nitrocellulose-coated bio-slides and displayed preservation of tissue morphology (Fig. S10). NeuN-positive cells (shown in red) have been visualized clearly on the spinal cord tissue sections. This indicates that bio-slides facilitate antibody penetration and antigen-antibody binding, similar to the binding observed on the microscopic glass slides (Fig. 8). Furthermore, confocal microscopy imaging confirmed that bio-slides enable high-resolution visualization of fluorescent neurons in the spinal cord tissue sections. Moreover, to demonstrate the performance of bio-slides in imaging thicker tissue sections, we performed fluorescence imaging on 30 µm spinal cord sections (Fig. S12).



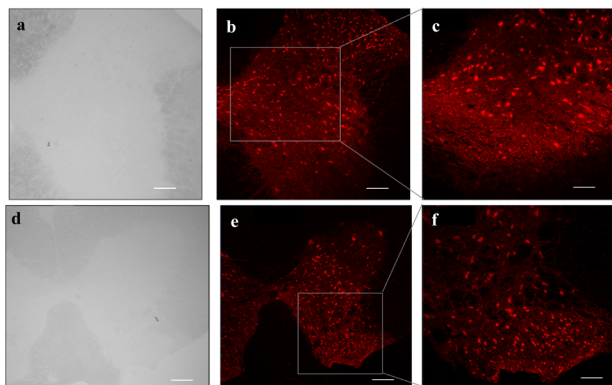


**Fig. 8** Immunohistochemical staining of spinal cord tissue sections on the bio-slide and glass slide. (a–c) Mouse spinal cord sections on bio-slides. (d–f) Mouse spinal cord sections on glass slides. (a and d) Transmitted light image at 10× magnification. (b and e) Anti-NeuN immunostaining at 10× magnification. (c and f) Anti-NeuN immunostaining at 20× magnification. Scale bar represents 100 μm.

These results highlight their versatility for both histological and cytological applications on par with glass slides (Fig. S13).

To account for minor surface irregularities on our bio-slides and to improve their performance in high-resolution imaging, we are currently doing surface engineering experiments. Also, we are planning to melt-down the scales and cast them into bio-slides using smooth moulds, exploiting the innate polymerizing ability of scales.

Collectively, these findings demonstrate that fish scales derived bio-slides are optically transparent, mechanically robust, and biologically compatible, supporting microscopy. Coupled with the custom 3D-printed adapter, they can be seamlessly integrated into existing laboratory workflows. Beyond their technical performance, bio-slides offer ecological and economic benefits by valorizing aquaculture waste into biodegradable laboratory tools, reducing dependence on energy-intensive glass production and aligning with circular economy principles.<sup>33–36</sup> With further refinements in uniformity, durability, and large-scale standardization, bio-slides hold promise as sustainable substitutes for glass slides in education, diagnostics, and biomedical research.

## 4 Conclusions

This study implements fish scale-derived bio-slides as a sustainable, biodegradable, and low-cost alternative to conventional glass slides for microscopy. Through simple etching and integration with a custom 3D-printed slide holder, the bio-slides exhibited excellent optical clarity, high transmittance, hydrophilicity and mechanical sturdiness, making them highly compatible with standard light/fluorescence microscopy and confocal platforms. Comparative imaging of plant and tissues sections, microorganisms, stained cells, and *in vitro* cultured cells confirmed that bio-slides deliver resolution and contrast equivalent to glass slides. Surface characterization further revealed tuneable wettability, offering flexibility for diverse biological applications. Importantly, bio-slides

address several limitations of conventional glass slides. Glass slides are energy-intensive to manufacture, brittle, and non-biodegradable, contributing to persistent laboratory waste. Their fragility makes them prone to shattering, producing sharp fragments that pose a significant safety hazard to laboratory personnel, particularly in teaching and clinical environments. In contrast, bio-slides not only valorize aquaculture waste but also provide biodegradability, surface tunability, reduced breakage risk, and overall safer handling, positioning them as a sustainable, safe and user-friendly alternative. The ability of bio-slides to seamlessly integrate into existing laboratory workflows underscores their translational potential in low-resource diagnostics, educational laboratories, and sustainable research practices cost-effectively. With future refinements in polishing, achieving surface uniformity, and scalable fabrication, bio-slides hold promise as a viable green substitute for glass slides, bridging ecological responsibility with scientific utility while reducing laboratory hazards.

## Author contributions

A. K. S. conceived the idea, planned and designed the research and experiments, provided laboratory, consumables, equipment and funding for the execution of the work, analyzed and interpreted the results, and wrote the manuscript (MS); D. S. P. conceived the idea and participated in initial discussions and experimental design. A. D. B., E. B. K., and A. R. performed the preliminary experiments and provided the raw data. A. M. E. and K. P. P. D. performed majority of the experiments and revisions, and prepared all images for the manuscript. V. S. K. performed sectioning of spinal cords and revision work on mouse spinal cords. J. F. V. A. and V. S. K. performed immunohistochemistry and confocal microscopy under the supervision of P. C. P. C. designed animal experiments and assisted in proof-reading the manuscript. C. K. and V. R. Y. participated in initial discussion. S. K. compiled the references for the MS. M. B. provided the resources for animal experiments and access for confocal microscopy.

## Conflicts of interest

The authors declare no conflict of interest.

## Data availability

All the data used in the manuscript are generated by us and will be made available upon request.

Supplementary information (SI) is available. See DOI: <https://doi.org/10.1039/d5fb00685f>.

## Acknowledgements

The authors thank SCIF and NRC, SRMIST, Chennai for instrument characterization.



## Notes and references

- 1 C. A. Noble, A. P. Biesemier, S. F. McClees, A. M. Alhussain, S. E. Helms and R. T. Brodell, The History of the Microscope Reflects Advances in Science and Medicine, *Semin. Diagn. Pathol.*, 2025, **42**(2), 150831, DOI: [10.1053/j.semmp.2024.01.002](https://doi.org/10.1053/j.semmp.2024.01.002).
- 2 Y. Wang, X. Zhang, J. Xu, X. Sun, X. Zhao, H. Li, Y. Liu, J. Tian, X. Hao, X. Kong, Z. Wang, J. Yang and Y. Su, The Development of Microscopic Imaging Technology and Its Application in Micro- and Nanotechnology, *Front. Chem.*, 2022, **10**, 931169, DOI: [10.3389/fchem.2022.931169](https://doi.org/10.3389/fchem.2022.931169).
- 3 J. S. H. Danial, Y. Aguib and M. H. Yacoub, Advanced Fluorescence Microscopy Techniques for the Life Sciences, *Global Cardiology Science and Practice*, 2016, **2016**(2), e201616, DOI: [10.21542/gcsp.2016.16](https://doi.org/10.21542/gcsp.2016.16).
- 4 H. Blom and H. Brismar, STED Microscopy: Increased Resolution for Medical Research?, *J. Intern. Med.*, 2014, **276**(6), 560–578, DOI: [10.1111/joim.12278](https://doi.org/10.1111/joim.12278).
- 5 Y. Chen, C.-P. Liang, Y. Liu, A. H. Fischer, A. V. Parwani and L. Pantanowitz, Review of Advanced Imaging Techniques, *J. Pathol. Inf.*, 2012, **3**(1), 22, DOI: [10.4103/2153-3539.96751](https://doi.org/10.4103/2153-3539.96751).
- 6 N. S. Vyas, M. Markow, C. Prieto-Granada, S. Gaudi, L. Turner, P. Rodriguez-Waitkus, J. L. Messina and D. M. Jukic, Comparing Whole Slide Digital Images versus Traditional Glass Slides in the Detection of Common Microscopic Features Seen in Dermatitis, *J. Pathol. Inf.*, 2016, **7**, 30, DOI: [10.4103/2153-3539.186909](https://doi.org/10.4103/2153-3539.186909).
- 7 Y. Liu, R. M. Levenson and M. W. Jenkins, Slide Over: Advances in Slide-Free Optical Microscopy as Drivers of Diagnostic Pathology, *Am. J. Pathol.*, 2022, **192**(2), 180–194, DOI: [10.1016/j.ajpath.2021.10.010](https://doi.org/10.1016/j.ajpath.2021.10.010).
- 8 L. M. Dowling, P. Roach, A. V. Rutter, I. Yousef, S. Pillai, D. Latham, D. G. van Pittius and J. Sulé-Suso, Optimization of Sample Preparation Using Glass Slides for Spectral Pathology, *Appl. Spectrosc.*, 2021, **75**(3), 343–350, DOI: [10.1177/0003702820945748](https://doi.org/10.1177/0003702820945748).
- 9 *The importance of coverslips in microscopy – 2022 – Wiley Analytical Science*, Analytical Science Article DO Series, <https://analyticalscience.wiley.com/content/article-do/importance-coverslips-microscopy>, accessed 2025-10-06.
- 10 Y. Sun, P. Ip and A. Chakrabarty, Simple Elimination of Background Fluorescence in Formalin-Fixed Human Brain Tissue for Immunofluorescence Microscopy, *J. Visualized Exp.*, 2017, **127**, 56188, DOI: [10.3791/56188](https://doi.org/10.3791/56188).
- 11 R. Zanini, G. Franceschin, E. Cattaruzza and A. Traviglia, A Review of Glass Corrosion: The Unique Contribution of Studying Ancient Glass to Validate Glass Alteration Models, *npj Mater. Degrad.*, 2023, **7**(1), 38, DOI: [10.1038/s41529-023-00355-4](https://doi.org/10.1038/s41529-023-00355-4).
- 12 Shubhava, A. Jayarama, G. K. Kannarpady, S. Kale, S. Prabhu and R. Pinto, Chemical Etching of Glasses in Hydrofluoric Acid: A Brief Review, *Mater. Today: Proc.*, 2022, **55**, 46–51, DOI: [10.1016/j.matpr.2021.12.110](https://doi.org/10.1016/j.matpr.2021.12.110).
- 13 A. Aliyo and A. Edin, Assessment of Safety Requirements and Their Practices Among Teaching Laboratories of Health Institutes, *Microbiol. Insights*, 2023, **16**, 11786361231174414, DOI: [10.1177/11786361231174414](https://doi.org/10.1177/11786361231174414).
- 14 G. Zhou, Y. Tian, F. Shi, C. Song, G. Tie, S. Liu, G. Zhou, J. Shao and Z. Wu, Scratch Morphology Transformation: An Alternative Method of Scratch Processing on Optical Surface, *Micromachines*, 2021, **12**(9), 1030, DOI: [10.3390/mi12091030](https://doi.org/10.3390/mi12091030).
- 15 Relevant-Buy-4667, *I cut myself. r/Histology*, [https://www.reddit.com/r/Histology/comments/149mwy0/i\\_cut\\_myself/](https://www.reddit.com/r/Histology/comments/149mwy0/i_cut_myself/), accessed 2025-10-06.
- 16 *Sharps Injury Prevention|Environmental Health and Safety – Office of the Vice President for Research|The University of Iowa*, <https://ehs.research.uiowa.edu/sharps-injury-prevention>, accessed 2025-10-06.
- 17 *Bloodborne Pathogens – Overview|Occupational Safety and Health Administration*, <https://www.osha.gov/bloodborne-pathogens>, accessed 2025-10-06.
- 18 E. Bontempi, G. P. Sorrentino, A. Zanoletti, I. Alessandri, L. E. Depero and A. Caneschi, Sustainable Materials and Their Contribution to the Sustainable Development Goals (SDGs): A Critical Review Based on an Italian Example, *Molecules*, 2021, **26**(5), 1407, DOI: [10.3390/molecules26051407](https://doi.org/10.3390/molecules26051407).
- 19 S. K. Wong, M. M. F. Yee, K.-Y. Chin and S. Ima-Nirwana, A Review of the Application of Natural and Synthetic Scaffolds in Bone Regeneration, *J. Funct. Biomater.*, 2023, **14**(5), 286, DOI: [10.3390/jfb14050286](https://doi.org/10.3390/jfb14050286).
- 20 M. Krishani, W. Y. Shin, H. Suhaimi and N. S. Sambudi, Development of Scaffolds from Bio-Based Natural Materials for Tissue Regeneration Applications: A Review, *Gels*, 2023, **9**(2), 100, DOI: [10.3390/gels9020100](https://doi.org/10.3390/gels9020100).
- 21 D. Qin, S. Bi, X. You, M. Wang, X. Cong, C. Yuan, M. Yu, X. Cheng and X.-G. Chen, Development and Application of Fish Scale Wastes as Versatile Natural Biomaterials, *Chem. Eng. J.*, 2022, **428**, 131102, DOI: [10.1016/j.cej.2021.131102](https://doi.org/10.1016/j.cej.2021.131102).
- 22 D. S. Parimi, C. S. Bhatt, T. K. Bollu, M. H. U, N. Jacob, M. Motapothula and A. K. Suresh, A Sustainable Transparent Biotemplate from Fish Scale Waste for Ultralow Volume High-Sensitive UV-Vis Spectroscopy, *Green Chem.*, 2021, **23**(20), 8217–8225, DOI: [10.1039/D1GC02569D](https://doi.org/10.1039/D1GC02569D).
- 23 Y. Shi, X. Zhang, R. Liu, X. Shao, Y. Zhao, Z. Gu and Q. Jiang, Self-Curling 3D Oriented Scaffolds from Fish Scales for Skeletal Muscle Regeneration, *Biomater. Res.*, 2022, **26**, 87, DOI: [10.1186/s40824-022-00335-w](https://doi.org/10.1186/s40824-022-00335-w).
- 24 D. Coppola, C. Lauritano, F. Palma Esposito, G. Riccio, C. Rizzo and D. de Pascale, Fish Waste: From Problem to Valuable Resource, *Mar. Drugs*, 2021, **19**(2), 116, DOI: [10.3390/md19020116](https://doi.org/10.3390/md19020116).
- 25 D. Qin, S. Bi, X. You, M. Wang, X. Cong, C. Yuan, M. Yu, X. Cheng and X.-G. Chen, Development and Application of Fish Scale Wastes as Versatile Natural Biomaterials, *Chem. Eng. J.*, 2022, **428**, 131102, DOI: [10.1016/j.cej.2021.131102](https://doi.org/10.1016/j.cej.2021.131102).
- 26 N. Tripathi, M. Zubair and A. Saprà, Gram Staining, in *StatPearls*, StatPearls Publishing, Treasure Island (FL), 2025.



- 27 P. M. Taylor, Biological Matrices and Bionanotechnology, *Philos. Trans. R. Soc., B*, 2007, **362**(1484), 1313–1320, DOI: [10.1098/rstb.2007.2117](https://doi.org/10.1098/rstb.2007.2117).
- 28 Y. Wang, S. E. Naleway and B. Wang, Biological and Bioinspired Materials: Structure Leading to Functional and Mechanical Performance, *Bioact. Mater.*, 2020, **5**(4), 745–757, DOI: [10.1016/j.bioactmat.2020.06.003](https://doi.org/10.1016/j.bioactmat.2020.06.003).
- 29 R. Praisie, D. Anandadurai, S. B. Nelson, S. Venkateshvaran and M. Thulasiram, Profile of Splash, Sharp and Needle-Stick Injuries Among Healthcare Workers in a Tertiary Care Hospital in Southern India, *Cureus*, 2023, **15**(7), e42671, DOI: [10.7759/cureus.42671](https://doi.org/10.7759/cureus.42671).
- 30 H. Feng, X. Li, X. Deng, X. Li, J. Guo, K. Ma and B. Jiang, The Lamellar Structure and Biomimetic Properties of a Fish Scale Matrix, *RSC Adv.*, 2020, 875–885, DOI: [10.1039/C9RA08189E](https://doi.org/10.1039/C9RA08189E).
- 31 E. Lizundia, F. Luzi and D. Puglia, Organic Waste Valorisation towards Circular and Sustainable Biocomposites, *Green Chem.*, 2022, **24**(14), 5429–5459, DOI: [10.1039/D2GC01668K](https://doi.org/10.1039/D2GC01668K).
- 32 I. S. Arvanitoyannis and A. Kassaveti, *Int. J. Food Sci. Technol.*, 2008, **8**, 726–745, DOI: [10.1111/j.1365-2621.2006.01513.x](https://doi.org/10.1111/j.1365-2621.2006.01513.x).
- 33 M. Shalaby, M. Agwa, H. Saeed, S. M. Khedr, O. Morsy and M. A. El-Demellawy, *J. Polym. Environ.*, 2020, **28**, 166–178, DOI: [10.1007/s10924-019-01594-w](https://doi.org/10.1007/s10924-019-01594-w).
- 34 C. H. Chou, Y. G. Chen, C. C. Lin, S. M. Lin, K. C. Yang and S. H. Chang, *Tissue Eng., Part A*, 2014, **20**, 2493–2502, DOI: [10.1089/ten.tea.2013.0174](https://doi.org/10.1089/ten.tea.2013.0174).
- 35 M. U. A. Khan, S. Ahmad and S. I. Butt, *Environ. Impact Assess. Rev.*, 2023, **102**, 1–5, DOI: [10.1016/j.eiar.2023.107195](https://doi.org/10.1016/j.eiar.2023.107195).
- 36 E. Battiston, F. Carollo, G. Tameni, E. Bernardo and A. Mazzi, *Ceramics*, 2025, **8**, 2–14, DOI: [10.3390/ceramics8030109](https://doi.org/10.3390/ceramics8030109).
- 37 J. Schindelin, I. Arganda-Carreras, E. Frise, V. Kaynig, M. Longair, T. Pietzsch, S. Preibisch, C. Rueden, S. Saalfeld, B. Schmid, J.-Y. Tinevez, D. J. White, V. Hartenstein, K. Eliceiri, P. Tomancak and A. Cardona, *Nat. Methods*, 2012, **9**, 676–682, DOI: [10.1038/nmeth.2019](https://doi.org/10.1038/nmeth.2019).

